The Canadian Mineralogist
Vol. 36, pp. x-xx (1998)

CLINOPYROXENE FROM LIPARI: COMPARISON WITH ANALOGUES FROM OTHER AEOLIAN ISLANDS, ITALY

DARIA PASQUAL[1] AND GIANMARIO MOLIN[1]

Dipartimento di Mineralogia e Petrologia, Università di Padova, Corso Garibaldi 37, I-35100 Padova, Italy

PIER FRANCESCO ZANAZZI[1]

Dipartimento di Scienze della Terra, Università di Perugia, Piazza Università, I-06100 Perugia, Italy

GINO MIROCLE CRISCI[1]

Dipartimento di Scienze della Terra, Università della Calabria, I-87036 Arcavacata di Rende-Cosenza, Italy

ABSTRACT

Clinopyroxene phenocrysts from the volcanic rocks of Lipari, one of the Aeolian Islands (Italy), were characterized by single-crystal X-ray diffraction and electron-microprobe analysis. They form three groups, related to different volcanic cycles. Although there is no evidence of tholeiitic rocks in the archipelago, the structural framework of these clinopyroxenes is close to those of clinopyroxene from subalkaline basalts of tholeiitic affinity. This feature may be ascribed to contamination of the magma by older gabbros in the lower crust, or to crystallization from an early magma of tholeiitic composition. Comparisons with analogues from other Aeolian Islands (Vulcano, Salina, Filicudi and Stromboli) highlight the fact that the Lipari clinopyroxene are low-pressure phenocrysts.

Keywords: clinopyroxene, crystal chemistry, volcanic rocks, pressure of crystallization, subalkaline, Lipari, Aeolian Islands.

SOMMAIRE

Nous avons caractérisé les phénocristaux de clinopyroxène des roches volcaniques de Lipari, une des îles éoliennes, en Italie, par diffraction X sur cristal unique et par analyse à la microsonde électronique. Ces phénocristaux forment trois groupes, selon le cycle d'activité volcanique. Quoiqu'il n'y ait pas de signes d'une activité tholéiitique dans cet archipel, la trame de ces échantillons de clinopyroxène ressemble à celle du clinopyroxène de basaltes subalcalins à affinité tholéiitique. On pourrait attribuer cette caractéristique à une contamination du magma par des gabbros plus anciens de la croûte inférieure, ou bien à la cristallisation d'une venue précoce de composition tholéiitique. Une comparaison avec des analogues sur les autres îles de l'archipel (Vulcano, Salina, Filicudi et Stromboli) souligne le fait que les phénocristaux de clinopyroxène de Lipari se sont formés à faible pression.

(Traduit par la Rédaction)

Mots-clés: clinopyroxène, chimie cristalline, roches volcaniques, pression de cristallisation, subalcalin, Lipari, îles éoliennes, Italie.

INTRODUCTION

Studies of Ca-rich pyroxenes from volcanic and mantle parageneses have revealed relations between the crystal chemistry of clinopyroxene and magma composition (Dal Negro *et al.* 1982, 1989). The aim of the present work is to characterize clinopyroxene from the island of Lipari, in the Aeolian Archipelago, southern Italy, as a function of the volcanic units of the area and the differentiation trends of the host rocks. The rocks of Lipari, all of subalkaline nature, include basaltic andesite, high-K andesite (HK-andesite), dacite and rhyolite. The Lipari lava flows show evidence of magma mixing and incorporation of basement rocks. Comparisons with analogues from other Aeolian Islands, Vulcano (Faraone *et al.* 1988), Salina and Filicudi (Malgarotto *et al.* 1993) and Stromboli (Pasqual *et al.* 1995), have been useful in characterizing the environments of crystallization in the individual magma chambers. Crystal-chemical investigations

[1] *E-mail addresses*: daria@dmp.unipd.it, molin@dmp.unipd.it, zanazzi@unipg.it, crisci@fis.unical.it

involved single-crystal X-ray diffraction (XRD) and electron-microprobe analysis (EMPA); the data permit an evaluation of the geometrical and chemical features of the clinopyroxene, and determination of accurate site-populations.

Geological Setting and Petrography

Lipari is the largest island of the Aeolian Archipelago; present volcanic activity is restricted to post-eruptive phenomena (low-temperature fumaroles and hot springs: Pichler 1980a, b). The ages of the volcanic products range from Pre-Tyrrhenian to late Roman times (223 ka – 580 A.D.: Crisci *et al.* 1991). The volcanic history of Lipari has been described in terms of ten cycles, identified on the basis of quiescent intervals, stratigraphic unconformities and compositional changes. The rocks from which the clinopyroxene phenocrysts were obtained belong to cycles II–VIII (Table 1) (Crisci *et al.* 1991). Thin sections of rock samples generally show phenocrysts of clinopyroxene, plagioclase and occasional orthopyroxene in a groundmass of plagioclase, clinopyroxene and glass. Sample L13 contains interstitial glass of rhyolitic composition (SiO_2 73.95 wt.%) in clinopyroxene phenocrysts, interpreted as due to reaction between felsic and basic melts (G.M. Crisci, pers. commun.). Petrography and bulk compositions were reported in Barker (1987) and Crisci *et al.* (1991).

TABLE 1. CLINOPYROXENE-BEARING SAMPLES, ERUPTIVE CYCLES, ROCK CLASSIFICATION AND LOCATION, LIPARI

	E.C.[1]	ROCK TYPE	LOCATION[2]
L2	II	Basaltic andesite	Acquacalda
L4	II	Basaltic andesite	P. del Legno Nero
L5	II	Basaltic andesite	P. del Legno Nero
L6	III	Basaltic andesite to HK-andesite[3]	Timpone Ospedale
L8	III	Basaltic andesite to HK-andesite	Chiesa Vecchia
L9	III	Basaltic andesite to HK-andesite	P. della Galera
L10	III	Basaltic andesite to HK-andesite	P. della Galera
L11	III	Basaltic andesite to HK-andesite	Monterosa
L12	IV	HK-andesite (cordierite-bearing)	Pietrovico
L16	IV	HK-andesite (cordierite-bearing)	Terme S. Calogero
L17	IV	HK-andesite (cordierite-bearing)	Terme S. Calogero
L18	IV	HK-andesite (cordierite-bearing)	Terme S. Calogero
L13	V-VI	HK-andesite	Costa d'Agosto
2L13	V-VI	HK-andesite	Costa d'Agosto
L13p	V-VI	HK-andesite	Costa d'Agosto
L14	V-VI	HK-andesite	Costa d'Agosto
L19	V-VI	HK-andesite	Monte S. Angelo
L20	V-VI	HK-andesite	Monte S. Angelo
2L20	V-VI	HK-andesite	Monte S. Angelo
L21	V-VI	HK-andesite	Monte S. Angelo
L22	VII-VIII	Rhyolite	Monte Guardia
2L22	VII-VIII	Rhyolite	Monte Guardia
L23	VII-VIII	Rhyolite	Monte Guardia
L24	VII-VIII	Rhyolite	Monte Guardia
L25	VII-VIII	Rhyolite	S. Nicola
L26	VII-VIII	Rhyolite	S. Nicola

[1] Eruptive cycle (E.C.) taken from Crisci *et al.* (1991). [2] See the geological map of Lipari (Pichler 1980). [3] HK-andesite: high-K andesite.

Experimental Methods

Twenty-seven untwinned crystals of clinopyroxene, ranging from 0.07 × 0.07 × 0.23 mm to 0.23 × 0.34 × 0.38 mm, were picked from rock sections about 100 mm thick. X-ray intensity data were obtained using a Philips PW 1100 four-circle automated diffractometer and graphite-monochromatized *MoK*$\bar{\alpha}$ ($\lambda = 0.7107$ Å). The equivalent $\pm hkl$ and $\pm h\bar{k}l$ reflections were measured in the range $2° < \theta < 30°$; as the mosaic spread of the crystals is quite large, the ω-scan mode was used. X-ray intensities were measured by step scan, scan width 1.6°, minimum and maximum measured times 0.4 and 0.8 s, respectively. Cell parameters were determined by the least-squares method applied to the θ values of about 60 reflections, measured with the LAT routine of the Philips diffractometer. Intensity data were corrected for Lorentz and polarization factors. An absorption correction was applied according to the semi-empirical method of North *et al.* (1968), and the values of the corrected intensities were merged to obtain a set of about 500 independent reflections having I greater than $3\sigma(I)$. Refinements were done in the space group *C2/c* without chemical constraints, starting from the atomic coordinates of diopside (Clark *et al.* 1969). Computations were done with the STRUCSY program (STOE copyright), which allows assignment of two scattering curves, f1 and f2, to each site, and refines occupancy factors x(f) with the constraint x(f1) + x(f2) = 1. The scattering curves for $Si^{2.5+}$, $O^{1.5-}$, Mg^{2+} and Fe^{2+} were used. Curves for partly ionized Si and O fit better the diffraction data, with $\sin\theta/\lambda \leq 0.3$ (Rossi *et al.* 1983). Atomic scattering curves were taken from the International Tables for X-ray Crystallography (1974) and Tokonami (1965). The electron density at the *M*2 site was calculated using a scattering curve obtained by linear combination of the Ca^{2+} and Na^{+} curves. Refinement allowed all parameters (atomic coordinates, anisotropic-displacement factors, site occupancies, scale factor and secondary extinction coefficient) to vary until the shifts were less than the least-squares difference of the corresponding parameters. In all crystals investigated, the final difference-Fourier map showed the presence of a residual electron density about 0.6 Å from the *M*2 site (site *M*2', assumed for Lipari clinopyroxenes to be occupied by Fe^{2+}; Rossi *et al.* 1987). Further least-squares refinement of both *M*2' occupancy and all other parameters in alternance converged to *R*-indices between 0.018 and 0.031. Bond lengths and geometrical parameters are reported in Table 2. Observed and calculated structure-factors and atomic coordinates are available from the authors or through the Depository of Unpublished Data, CISTI, National Research Council of Canada, Ottawa, Ontario K1A 0S2.

The same single crystals were used for chemical analysis using a CAMECA CAMEBAX electron microprobe with a wavelength-dispersion system (WDS) operating with a ~1 μm beam at 15 kV and

TABLE 2. STRUCTURAL PARAMETERS, BOND LENGTHS (Å), VOLUMES (Å^3) AND ANGLES (°), CLINOPYROXENE SUITE FROM LIPARI

	L2	L4	L5	L6	L8	L9	L10	L11	L12	L13	2L13	L13p	L14
a	9.740(5)	9.737(8)	9.740(5)	9.738(7)	9.740(6)	9.740(6)	9.739(7)	9.739(6)	9.749(11)	9.747(4)	9.747(10)	9.751(7)	9.743(5)
b	8.911(4)	8.912(8)	8.910(3)	8.911(4)	8.923(4)	8.918(4)	8.916(4)	8.915(4)	8.925(9)	8.921(3)	8.928(6)	8.938(4)	8.924(4)
c	5.253(2)	5.254(4)	5.255(2)	5.257(3)	5.257(3)	5.257(2)	5.259(3)	5.259(3)	5.257(4)	5.260(3)	5.259(5)	5.257(3)	5.260(3)
β	106.13(4)	106.21(6)	106.18(4)	106.27(5)	106.38(5)	106.42(4)	106.43(5)	106.36(5)	106.20(8)	106.23(4)	106.31(8)	106.27(5)	106.32(4)
V cell	438.05	437.82	437.94	437.84	438.36	438.03	438.03	438.12	439.30	439.14	439.27	439.83	438.90
R_{obs} %*	2.06	1.99	2.08	1.95	2.66	2.23	2.60	2.17	3.13	2.30	2.98	2.59	2.62
*M*1 site													
*M*1–O2	2.047(2)	2.047(2)	2.045(2)	2.046(2)	2.047(2)	2.047(2)	2.045(2)	2.044(2)	2.049(3)	2.044(2)	2.046(3)	2.053(2)	2.048(2)
*M*1–O1$_{A2}$	2.056(2)	2.057(2)	2.056(2)	2.056(2)	2.061(2)	2.059(2)	2.058(2)	2.057(2)	2.066(3)	2.063(2)	2.066(3)	2.069(2)	2.065(2)
*M*1–O1$_{A1}$	2.128(2)	2.131(2)	2.130(2)	2.133(2)	2.137(2)	2.138(2)	2.135(2)	2.138(2)	2.134(3)	2.139(2)	2.142(3)	2.142(2)	2.139(2)
Mean	2.077(3)	2.079(3)	2.077(3)	2.078(3)	2.082(3)	2.082(3)	2.079(3)	2.080(3)	2.083(5)	2.082(3)	2.085(5)	2.088(3)	2.084(3)
Volume	11.857(5)	11.886(4)	11.859(4)	11.875(6)	11.945(8)	11.937(7)	11.892(5)	11.901(6)	11.964(11)	11.944(5)	11.990(10)	12.051(6)	11.982(8)
*M*2 site													
*M*2–O2	2.309(2)	2.301(2)	2.307(2)	2.296(2)	2.274(2)	2.271(2)	2.290(2)	2.279(2)	2.295(4)	2.278(2)	2.277(3)	2.277(3)	2.277(2)
*M*2–O1	2.344(2)	2.340(2)	2.342(2)	2.337(2)	2.316(2)	2.315(2)	2.331(2)	2.320(2)	2.330(3)	2.318(2)	2.317(3)	2.316(2)	2.316(2)
*M*2–O3$_{C1}$	2.579(2)	2.584(2)	2.581(2)	2.589(2)	2.612(2)	2.612(2)	2.591(2)	2.604(2)	2.603(3)	2.613(2)	2.616(3)	2.616(2)	2.613(2)
*M*2–O3$_{C2}$	2.730(2)	2.735(2)	2.733(2)	2.736(2)	2.755(2)	2.756(2)	2.745(2)	2.751(2)	2.741(3)	2.757(2)	2.754(3)	2.760(2)	2.755(2)
Mean	2.491(4)	2.490(4)	2.491(4)	2.490(4)	2.489(4)	2.489(4)	2.489(4)	2.489(4)	2.492(7)	2.491(4)	2.491(6)	2.492(5)	2.490(4)
Volume	25.480(8)	25.445(6)	25.476(7)	25.422(8)	25.317(12)	25.300(10)	25.381(9)	25.318(9)	25.480(16)	25.376(8)	25.377(15)	25.396(10)	25.365(11)
T site													
T–O2	1.591(2)	1.590(2)	1.590(2)	1.591(2)	1.594(2)	1.593(2)	1.592(2)	1.593(2)	1.593(3)	1.595(2)	1.596(3)	1.591(2)	1.594(2)
T–O1	1.607(2)	1.606(2)	1.609(2)	1.608(2)	1.610(2)	1.611(2)	1.609(2)	1.613(2)	1.610(3)	1.614(2)	1.610(3)	1.609(2)	1.610(2)
T–O3$_{A1}$	1.665(2)	1.664(2)	1.663(2)	1.663(1)	1.662(2)	1.662(2)	1.666(2)	1.662(2)	1.662(3)	1.660(2)	1.664(3)	1.663(2)	1.662(2)
T–O3$_{A2}$	1.682(2)	1.681(2)	1.682(2)	1.682(2)	1.680(2)	1.677(2)	1.678(2)	1.680(2)	1.685(3)	1.682(2)	1.679(3)	1.678(2)	1.680(2)
T–O$_{br}$	1.673	1.673	1.673	1.672	1.671	1.669	1.672	1.671	1.673	1.671	1.671	1.670	1.671
T–O$_{no\ br}$	1.599	1.598	1.599	1.600	1.602	1.602	1.600	1.603	1.601	1.604	1.603	1.600	1.602
Mean	1.636(4)	1.635(4)	1.636(4)	1.636(4)	1.636(4)	1.636(4)	1.636(4)	1.637(4)	1.637(6)	1.638(4)	1.637(6)	1.635(4)	1.637(4)
Volume	2.230(2)	2.226(2)	2.229(2)	2.229(3)	2.232(4)	2.229(4)	2.231(2)	2.233(3)	2.236(6)	2.236(2)	2.236(5)	2.227(3)	2.233(4)

	L16	L17	L18	L19	L20	2L20	L21	L22	2L22	L23	L24	L25	L26
a	9.751(8)	9.748(6)	9.746(6)	9.746(5)	9.751(5)	9.749(5)	9.745(4)	9.751(5)	9.753(6)	9.748(5)	9.749(6)	9.743(6)	9.743(4)
b	8.935(4)	8.928(4)	8.925(4)	8.932(3)	8.932(3)	8.929(3)	8.924(3)	8.910(3)	8.920(4)	8.915(3)	8.913(4)	8.914(4)	8.910(3)
c	5.255(3)	5.259(3)	5.258(2)	5.258(2)	5.256(2)	5.257(2)	5.258(2)	5.269(2)	5.266(3)	5.264(2)	5.264(2)	5.260(3)	5.258(2)
β	106.27(6)	106.29(5)	106.27(4)	106.41(4)	106.22(3)	106.19(4)	106.28(3)	106.07(4)	106.09(4)	106.11(3)	106.07(4)	106.21(4)	106.22(3)
V cell	439.55	439.31	439.00	439.08	439.64	439.44	438.99	439.83	440.18	439.52	439.52	438.70	438.30
R_{obs} %*	2.47	2.39	2.06	2.28	2.40	2.47	2.24	1.76	2.57	1.86	2.62	2.24	2.17
*M*1 site													
*M*1–O2	2.052(2)	2.048(2)	2.049(2)	2.050(2)	2.051(2)	2.051(2)	2.048(2)	2.040(1)	2.045(2)	2.041(2)	2.041(2)	2.044(2)	2.044(2)
*M*1–O2$_{A2}$	2.067(2)	2.064(2)	2.062(2)	2.065(2)	2.063(2)	2.065(2)	2.062(2)	2.061(2)	2.066(2)	2.061(2)	2.061(2)	2.058(2)	2.058(2)
*M*1–O2$_{A1}$	2.142(2)	2.140(2)	2.138(2)	2.142(2)	2.140(2)	2.136(2)	2.140(2)	2.129(1)	2.135(2)	2.132(1)	2.132(2)	2.133(2)	2.134(2)
Mean	2.087(3)	2.084(3)	2.083(3)	2.086(3)	2.085(3)	2.084(3)	2.083(3)	2.077(2)	2.082(3)	2.078(3)	2.078(3)	2.079(3)	2.079(3)
Volume	12.035(6)	11.975(6)	11.959(5)	12.014(5)	11.994(6)	11.975(6)	11.965(8)	11.846(5)	11.946(9)	11.875(4)	11.869(7)	11.880(5)	11.886(5)
*M*2 site													
*M*2–O2	2.278(3)	2.282(2)	2.287(2)	2.263(2)	2.286(2)	2.290(2)	2.281(2)	2.324(2)	2.312(3)	2.315(2)	2.322(3)	2.304(2)	2.300(2)
*M*2–O1	2.319(2)	2.320(2)	2.326(2)	2.307(2)	2.325(2)	2.329(2)	2.322(2)	2.352(1)	2.345(2)	2.345(1)	2.348(2)	2.340(2)	2.339(2)
*M*2–O3$_{C1}$	2.615(2)	2.609(2)	2.603(2)	2.627(2)	2.607(2)	2.603(2)	2.607(2)	2.576(1)	2.582(2)	2.581(2)	2.577(2)	2.585(2)	2.584(2)
*M*2–O3$_{C2}$	2.759(2)	2.756(2)	2.750(2)	2.768(2)	2.752(2)	2.748(2)	2.753(2)	2.727(1)	2.735(2)	2.733(2)	2.729(2)	2.738(2)	2.737(2)
Mean	2.493(5)	2.492(4)	2.491(4)	2.491(4)	2.493(4)	2.493(4)	2.491(4)	2.495(3)	2.493(5)	2.494(4)	2.494(5)	2.492(4)	2.490(4)
Volume	25.422(10)	25.406(9)	25.422(8)	25.317(8)	25.453(11)	25.470(10)	25.386(11)	25.630(7)	25.567(13)	25.571(7)	25.613(11)	25.498(8)	25.443(9)
T site													
T–O2	1.592(2)	1.593(2)	1.592(2)	1.594(2)	1.593(2)	1.592(2)	1.595(2)	1.596(1)	1.596(2)	1.595(1)	1.595(2)	1.592(2)	1.592(2)
T–O1	1.608(2)	1.612(2)	1.610(2)	1.611(2)	1.610(2)	1.609(2)	1.609(2)	1.614(1)	1.609(2)	1.612(2)	1.611(2)	1.610(2)	1.609(2)
T–O3$_{A1}$	1.661(2)	1.661(2)	1.663(2)	1.661(2)	1.661(2)	1.662(2)	1.663(2)	1.667(1)	1.665(2)	1.664(1)	1.665(2)	1.663(2)	1.662(2)
T–O3$_{A2}$	1.680(2)	1.681(2)	1.680(2)	1.677(2)	1.681(2)	1.682(2)	1.678(2)	1.686(1)	1.686(2)	1.686(1)	1.686(2)	1.684(2)	1.683(2)
T–O$_{br}$	1.670	1.671	1.671	1.669	1.671	1.672	1.671	1.676	1.676	1.675	1.676	1.674	1.673
T–O$_{no\ br}$	1.600	1.603	1.601	1.602	1.601	1.601	1.602	1.605	1.602	1.603	1.603	1.601	1.600
Mean	1.635(4)	1.637(4)	1.636(4)	1.636(4)	1.636(4)	1.636(4)	1.636(4)	1.641(2)	1.639(4)	1.639(3)	1.639(4)	1.637(4)	1.637(4)
Volume	2.227(2)	2.234(2)	2.230(2)	2.229(2)	2.231(3)	2.231(2)	2.231(4)	2.248(3)	2.241(5)	2.243(2)	2.243(3)	2.235(2)	2.232(2)

* R_{obs} % = observed discrepancy factor (× 100) expressed as $\Sigma||F_o| - |F_c||/\Sigma|F_o|$.

15 nA, with peak and background counting times of 20 s. Synthetic pure oxides were used as standards for Mg, Al, Ti, Cr, Mn and Fe, and wollastonite and albite were used for Si, Ca and Na. X-ray counts were converted to oxide weight percentages using the PAP (CAMECA) correction program. Single-crystal compositions are generally averaged from seven or more spots (Table 3).

Site populations (Table 4) were calculated using the results of structural refinement and electron-microprobe analysis, as described by Faraone *et al.* (1988).

TABLE 3. AVERAGE COMPOSITION OF CLINOPYROXENE SAMPLES, LIPARI SUITE (ELECTRON-MICROPROBE DATA, WITH ESTIMATED STANDARD DEVIATIONS)

	L2	L4	L5	L6	L8	L9	L10	L11	L12	L13	2L13	L13p	L14
SiO_2	53.99(32)	53.88(61)	52.75(14)	53.20(53)	52.25(14)	51.71(32)	51.44(33)	52.89(38)	51.40(34)	51.03(83)	50.73(48)	51.44(42)	50.88(28)
TiO_2	0.17(2)	0.16(5)	0.18(3)	0.25(4)	0.45(2)	0.43(4)	0.46(2)	0.35(3)	0.55(2)	0.47(13)	0.63(5)	0.48(3)	0.63(3)
Al_2O_3	1.68(3)	1.66(43)	1.85(5)	2.30(16)	1.81(17)	2.42(30)	2.55(9)	2.40(10)	2.37(7)	3.34(27)	2.21(14)	1.41(15)	2.53(5)
Cr_2O_3	0.22(8)	0.77(25)	0.17(4)	0.17(7)	0.01(3)	0.04(5)	0.01(1)	0.05(3)	0.02(3)	0.04(3)	0.02(2)	0.03(3)	0.06(2)
FeO	4.30(10)	4.00(89)	4.48(4)	5.06(34)	10.19(25)	10.50(51)	9.92(67)	7.81(37)	10.83(15)	9.96(68)	14.26(90)	12.86(25)	12.62(20)
MnO	0.16(5)	0.13(5)	0.08(3)	0.16(7)	0.39(6)	0.30(4)	0.31(5)	0.25(5)	0.26(4)	0.31(5)	0.40(6)	0.45(4)	0.35(8)
MgO	16.91(14)	18.07(83)	16.60(12)	16.71(23)	15.29(10)	15.23(42)	15.43(10)	15.68(22)	13.85(9)	14.10(38)	13.55(48)	13.19(9)	13.39(22)
CaO	23.02(21)	21.79(48)	22.89(18)	21.78(49)	19.56(23)	19.12(40)	19.45(52)	21.76(57)	20.65(26)	21.08(42)	18.22(160)	19.25(20)	19.38(25)
Na_2O	0.12(3)	0.13(2)	0.16(3)	0.15(4)	0.21(3)	0.21(3)	0.18(4)	0.14(3)	0.24(3)	0.28(1)	0.25(5)	0.22(2)	0.28(3)
Total	100.57(41)	100.59(40)	99.15(44)	99.78(68)	100.16(14)	99.96(24)	99.75(67)	101.33(47)	100.17(47)	100.61(41)	100.27(50)	99.33(51)	100.12(43)

	L16	L17	L18	L19	L20	2L20	L21	L22	2L22	L23	L24	L25	L26
SiO_2	51.50(36)	51.48(42)	51.48(42)	50.88(59)	51.85(25)	52.17(20)	51.18(23)	49.98(58)	50.84(31)	51.02(54)	51.00(10)	52.24(39)	51.47(43)
TiO_2	0.43(5)	0.58(5)	0.54(2)	0.59(5)	0.46(2)	0.44(5)	0.52(5)	0.70(16)	0.62(5)	0.62(3)	0.61(4)	0.36(9)	0.40(7)
Al_2O_3	1.38(16)	2.25(23)	2.14(26)	1.90(10)	1.40(13)	1.55(6)	2.24(9)	3.75(52)	4.39(7)	3.21(30)	3.09(18)	2.35(21)	2.46(27)
Cr_2O_3	0.03(4)	0.03(3)	0.04(3)	0.06(5)	0.04(2)	0.01(1)	0.03(3)	0.03(3)	0.05(2)	0.01(1)	0.03(4)	0.04(6)	0.14(13)
FeO	12.29(29)	12.51(30)	10.77(40)	14.00(19)	10.74(77)	10.73(28)	11.68(86)	9.08(45)	7.41(33)	9.89(45)	8.72(15)	7.92(77)	7.93(67)
MnO	0.45(7)	0.42(8)	0.34(4)	0.41(5)	0.48(5)	0.37(2)	0.33(6)	0.40(7)	0.17(4)	0.31(4)	0.25(4)	0.23(4)	0.21(5)
MgO	13.54(13)	13.29(20)	14.17(17)	13.48(39)	13.73(12)	14.46(16)	13.68(37)	13.17(46)	13.98(7)	13.76(33)	13.55(33)	15.51(28)	14.85(27)
CaO	19.34(22)	19.58(19)	20.07(41)	18.34(22)	20.65(47)	20.65(18)	19.24(105)	21.91(28)	22.70(15)	21.88(18)	22.54(4)	21.47(55)	21.60(48)
Na_2O	0.25(2)	0.28(4)	0.23(2)	0.25(4)	0.18(5)	0.22(3)	0.24(3)	0.45(4)	0.37(5)	0.39(3)	0.34(5)	0.35(3)	0.34(3)
Total	99.21(67)	100.42(40)	99.78(47)	99.91(95)	99.53(36)	100.60(22)	99.14(38)	99.47(50)	100.53(61)	101.09(71)	100.11(27)	100.47(46)	99.40(43)

Compositions are expressed in wt.% oxides.

Crystal Chemistry

Unlike the clinopyroxene samples of the other Aeolian Islands, which show two main compositions, diopsidic and augitic, most clinopyroxene crystals from Lipari are augitic (Fig. 1). The crystal-chemical behavior of the Lipari clinopyroxene follows the general trends observed for clinopyroxene from magmatic rocks (Dal Negro *et al.* 1982, Carbonin *et al.* 1984). On the basis of structural features, three groups may be distinguished and related to the seven cycles (II–VIII) of volcanic rock sampled. The volume of the *M*1 polyhedron *V*(*M*1) *versus* the cell volume *V*(cell) (Fig. 2) highlights this feature; in the inset, the relationship between volume of the *M*1 site and its content of Fe^{2+} is shown. Group A has the lowest values of *V*(*M*1) and low values for *V*(cell) owing to low Fe^{2+}(*M*1) content, and comprises clinopyroxene from early volcanic cycles (II–III, Table 1). Group B comprises crystals from intermediate cycles (IV–VI), with the highest *V*(cell) and *V*(*M*1), in accord with the higher content of Fe^{2+}(*M*1) and the more evolved character of the magmas. Group C comprises crystals from xenoliths occurring in the rhyolites of the Monte Guardia cycles (VII–VIII). Group-C crystals are characterized by low *V*(*M*1), because of their high content of trivalent ions, mainly Fe^{3+} and $^{[6]}Al$, and by a wide range of *V*(cell), mainly due to variations in Ca content at the *M*2 site (up to 0.90 atoms per formula unit).

A plot of β *versus* *V*(*M*2)/*V*(*M*1) (Dal Negro *et al.* 1989) distinguishes clinopyroxene from various petrogenetic environments (Fig. 3), as the geometrical parameter β and the ratio *V*(*M*2)/*V*(*M*1) generally are related to 1/Fe^{2+}(*M*1) and to (Ca + Na) content, respectively (see inset). From this point of view, groups A and B fall in the field of clinopyroxenes from subalkaline basalts [lowest *V*(*M*2)/*V*(*M*1) values and highest ß-values, owing to lowest contents of Ca and Fe^{2+} at the

TABLE 4. SITE PARTITIONING IN CLINOPYROXENE FROM LIPARI, EXPRESSED IN ATOMS PER FORMULA UNIT ($M1M2T_2O_6$)

	L2	L4	L5	L6	L8	L9	L10	L11	L12	L13	2L13	L13p	L14
T site													
Si	1.961(10)	1.950(14)	1.944(6)	1.949(7)	1.940(5)	1.924(12)	1.913(7)	1.928(11)	1.919(7)	1.888(21)	1.909(18)	1.953(10)	1.911(10)
$^{[4]}$Al	0.039(10)	0.050(14)	0.056(6)	0.051(7)	0.060(5)	0.076(12)	0.087(7)	0.072(11)	0.081(7)	0.112(21)	0.091(18)	0.047(10)	0.089(10)
*M*1 site													
Mg	0.857(7)	0.896(40)	0.861(5)	0.854(11)	0.829(5)	0.805(22)	0.757(9)	0.835(12)	0.733(4)	0.764(20)	0.717(28)	0.721(7)	0.722(10)
Fe^{2+}	0.099(18)	0.050(23)	0.075(13)	0.086(11)	0.108(10)	0.115(24)	0.156(17)	0.093(23)	0.184(9)	0.118(19)	0.191(53)	0.229(12)	0.186(20)
$^{[6]}$Al	0.033(10)	0.020(7)	0.024(8)	0.048(3)	0.019(3)	0.030(8)	0.025(7)	0.031(9)	0.023(7)	0.034(14)	0.007(13)	0.017(9)	0.024(8)
Fe^{3+}	0.000	0.008(6)	0.030(13)	0.000(2)	0.031(2)	0.037(14)	0.049(13)	0.030(19)	0.044(12)	0.070(29)	0.066(28)	0.018(17)	0.048(18)
Ti	0.005(0)	0.004(2)	0.005(1)	0.007(1)	0.013(0)	0.012(1)	0.013(1)	0.010(1)	0.015(1)	0.013(4)	0.018(2)	0.014(1)	0.018(1)
Cr	0.006(3)	0.022(7)	0.005(1)	0.005(2)	0.000(1)	0.001(1)	0.000(0)	0.001(1)	0.001(1)	0.001(1)	0.001(1)	0.001(1)	0.002(1)
*M*2 (+*M*2') site													
Ca	0.896(7)	0.845(22)	0.903(4)	0.855(13)	0.778(9)	0.762(16)	0.775(19)	0.850(22)	0.826(8)	0.836(6)	0.735(64)	0.783(6)	0.780(10)
Na	0.008(2)	0.008(2)	0.012(2)	0.011(3)	0.015(2)	0.015(2)	0.013(3)	0.010(2)	0.017(2)	0.020(1)	0.018(4)	0.016(2)	0.020(2)
Mn	0.005(2)	0.004(1)	0.003(1)	0.005(3)	0.012(2)	0.009(1)	0.010(2)	0.008(2)	0.008(1)	0.010(2)	0.013(2)	0.014(1)	0.011(3)
Mg	0.059(7)	0.079(40)	0.051(5)	0.058(11)	0.017(5)	0.039(22)	0.098(9)	0.017(12)	0.038(4)	0.014(20)	0.043(28)	0.025(7)	0.027(10)
Fe^{2+}	0.032(18)	0.064(23)	0.033(13)	0.071(11)	0.178(10)	0.175(24)	0.104(17)	0.115(23)	0.111(9)	0.120(19)	0.191(53)	0.162(12)	0.162(20)
Σ1	32.63(28)	32.68(23)	32.94(25)	33.21(23)	34.95(42)	35.13(33)	34.60(31)	34.81(32)	35.23(45)	34.79(34)	36.22(51)	36.32(43)	35.90(39)
Σ2	33.21(5)	32.84(42)	33.34(6)	33.27(15)	34.95(8)	34.94(20)	34.80(17)	34.37(13)	35.63(10)	35.29(36)	36.50(22)	36.32(12)	36.13(10)

	L16	L17	L18	L19	L20	2L20	L21	L22	2L22	L23	L24	L25	L26
Si	1.952(4)	1.929(14)	1.928(9)	1.922(6)	1.953(3)	1.937(6)	1.936(6)	1.871(16)	1.870(5)	1.881(11)	1.895(8)	1.918(10)	1.915(12)
$^{[4]}$Al	0.048(4)	0.071(14)	0.072(9)	0.078(6)	0.047(3)	0.063(6)	0.064(6)	0.129(16)	0.130(5)	0.119(11)	0.105(8)	0.082(10)	0.085(12)
*M*1 site													
Mg	0.750(8)	0.723(11)	0.769(10)	0.743(16)	0.758(8)	0.781(8)	0.741(21)	0.719(5)	0.743(5)	0.736(16)	0.733(16)	0.809(15)	0.792(13)
Fe^{2+}	0.197(15)	0.202(25)	0.158(17)	0.178(11)	0.195(16)	0.153(18)	0.191(22)	0.139(12)	0.118(14)	0.135(9)	0.155(26)	0.095(37)	0.108(27)
$^{[6]}$Al	0.013(8)	0.029(7)	0.022(9)	0.006(7)	0.015(8)	0.005(7)	0.036(7)	0.036(3)	0.061(6)	0.020(5)	0.030(13)	0.020(10)	0.023(9)
Fe^{3+}	0.027(11)	0.029(18)	0.035(14)	0.054(11)	0.018(9)	0.049(13)	0.016(13)	0.085(15)	0.060(11)	0.092(11)	0.064(22)	0.065(19)	0.062(15)
Ti	0.012(1)	0.016(2)	0.015(1)	0.017(1)	0.013(1)	0.012(1)	0.015(2)	0.020(1)	0.017(1)	0.017(1)	0.017(1)	0.010(2)	0.011(2)
Cr	0.001(1)	0.001(1)	0.001(1)	0.002(2)	0.001(1)	0.000(0)	0.001(1)	0.001(1)	0.001(1)	0.000(1)	0.001(1)	0.001(2)	0.004(4)
*M*2 (+*M*2') site													
Ca	0.786(10)	0.786(8)	0.805(15)	0.742(15)	0.833(16)	0.822(7)	0.780(42)	0.879(7)	0.895(8)	0.864(4)	0.897(3)	0.845(22)	0.861(17)
Na	0.018(2)	0.020(3)	0.017(2)	0.018(3)	0.013(4)	0.016(2)	0.018(3)	0.033(3)	0.026(4)	0.028(3)	0.024(4)	0.025(3)	0.025(2)
Mn	0.014(2)	0.013(2)	0.011(1)	0.013(1)	0.015(2)	0.012(1)	0.011(2)	0.013(3)	0.005(1)	0.010(1)	0.008(2)	0.007(1)	0.007(2)
Mg	0.015(8)	0.019(11)	0.022(10)	0.016(16)	0.013(8)	0.019(8)	0.030(21)	0.016(5)	0.023(5)	0.020(16)	0.019(16)	0.040(15	0.030(13)
Fe^{2+}	0.167(15)	0.162(25)	0.145(17)	0.211(11)	0.126(16)	0.131(18)	0.161(22)	0.059(12)	0.051(14)	0.078(9)	0.052(26)	0.083(37)	0.077(27)
Σ1	36.02(41)	35.93(39)	35.36(33)	36.35(35)	35.40(44)	35.17(41)	35.43(38)	34.95(21)	35.06(36)	35.04(23)	34.75(37)	33.99(27)	34.19(29)
Σ2	36.07(8)	36.13(9)	35.48(9)	36.49(16)	35.75(23)	35.50(11)	35.71(12)	35.38(22)	34.65(13)	35.47(20)	35.26(8)	34.36(19)	34.59(17)

Σ1: Σe^-_{str} = number of electrons resulting in *M*1 + *M*2 sites from structural refinement.
Σ2: Σe^-_{ch} = number of electrons resulting in *M*1 + *M*2 sites calculated from results of chemical analysis.

*M*2 and *M*1 sites, respectively]. Because of their high Ca, $^{[6]}$Al and Fe^{3+} contents, group-C crystals show structural configurations related to clinopyroxene from alkaline rocks (Dal Negro *et al.* 1989).

Discussion and Conclusions

Comparisons of clinopyroxene from Lipari with analogues from Vulcano, Salina, Filicudi and Stromboli highlight the main differences in plots of *V*(*M*1) *versus* *V*(cell) and ß-angle *versus* *V*(*M*2)/*V*(*M*1) (Figs. 4, 5). *V*(cell) and *V*(*M*1) are affected by pressure during crystallization (Manoli & Molin 1988, Dal Negro *et al.* 1989, Nimis 1995). It follows that the plot of *V*(*M*1) *versus* *V*(cell) (Fig. 4) may distinguish clinopyroxene samples with similar Mg/Fe but that crystallized at different pressures. Note that the clinopyroxene at Filicudi approaches the field of high pressure, represented by clinopyroxene megacrysts crystallized in the stability field of spinel from alkaline rocks (Dal Negro *et al.*

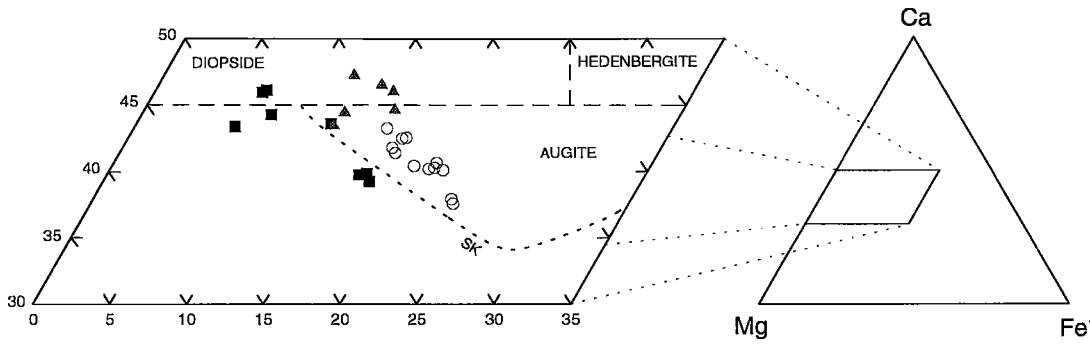

FIG. 1. Composition of clinopyroxene in terms of Ca–Mg–Fe* (Fe* = Fe^{2+} + Fe^{3+} + Mn); squares: group A, circles: group B, triangles: group C; SK: Skaergaard clinopyroxene variation.

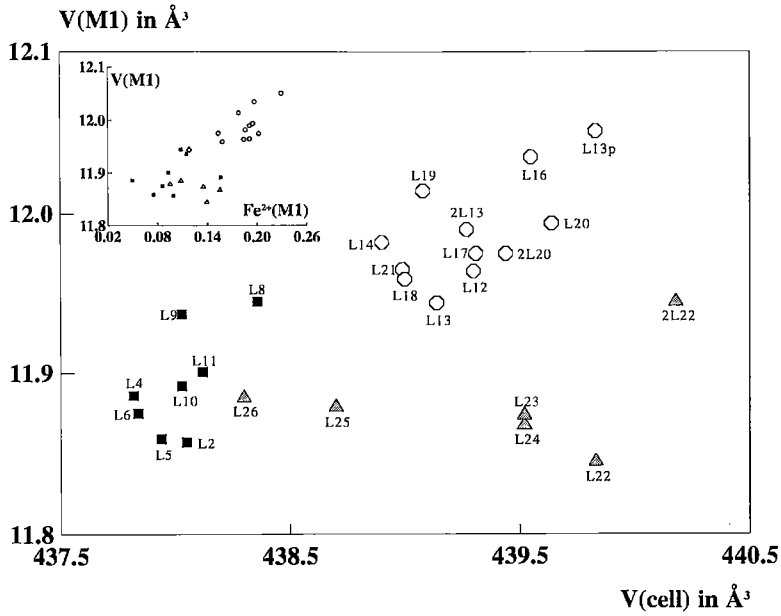

FIG. 2. *M*1 site volume *V*(*M*1) *versus* cell volume *V*(cell) in clinopyroxene; in the inset, the *V*(*M*1) *versus* Fe^{2+}(*M*1) content; symbols as in Figure 1.

1989), clinopyroxene from spinel lherzolitic nodules (Dal Negro *et al.* 1984) and by the 190/3 clinopyroxene synthetized at 12 kbar from the 74275 lunar basalt (Manoli & Molin 1988). Petrological and geochemical data suggest that at Filicudi, the clinopyroxene crystallized at relatively high pressure, indicating that the host magmas originated at the greatest depths relative to the other batches of basic melt in the Aeolian Archipelago (Malgarotto *et al.* 1993). In contrast, the clinopyroxene at Lipari plots in the low-pressure field, and crystallized from fairly evolved magmas, which may have experienced crustal assimilation.

The β *versus* *V*(*M*2)/*V*(*M*1) plot (Fig. 5) shows that the structural features of the clinopyroxene at Lipari (groups A and B) are close to those of clinopyroxene from subalkaline basalts, suggesting, by comparison with analogues of tholeiites of the Central Ethiopian Plateau (Dal Negro *et al.* 1982), a tholeiitic affinity. This compositional shift toward the subalkaline field is markedly different from trends in the suite of clinopyroxene from Stromboli, which plots in the field of alkaline magmas (high-K and shoshonitic: Pasqual *et al.* 1995) and from the Sunda arc volcanic rocks (Salviulo & Molin 1993). Even if tholeiitic rocks are

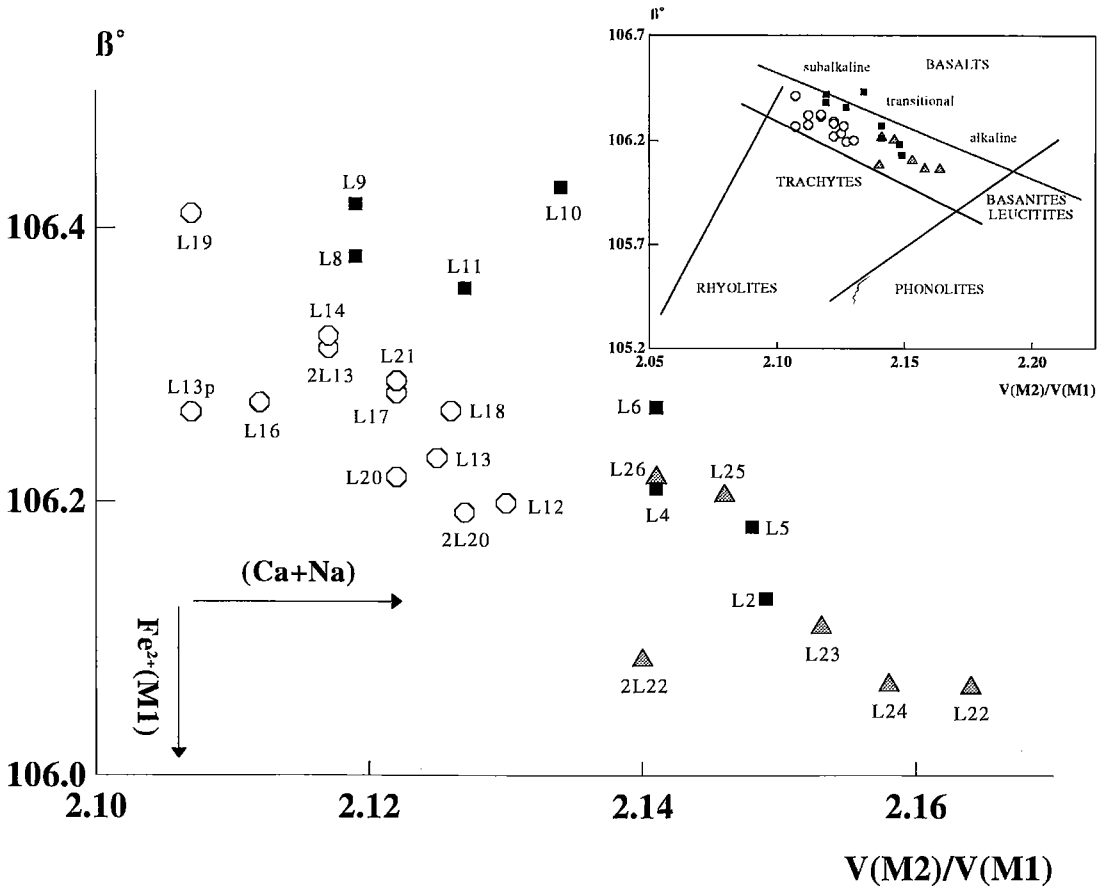

FIG. 3. The angle β angle *versus* volume ratio of *M*2 and *M*1 sites [*V*(*M*2)/*V*(*M*1)]; symbols as in Figure 1. Inset according to Dal Negro *et al.* (1989).

absent in the Lipari suite, the existence of arc-tholeiitic basalts in the Aeolian Seamounts (Lametini volcano: Beccaluva *et al.* 1985) and the conclusions of geological and petrological studies (Barker 1987, Crisci *et al.* 1991), show that such crystallographic evidence may be interpreted in two ways: (1) the clinopyroxene crystals are the product of contamination of magma by pre-existing gabbroic rocks in the lower crust, or (2) they crystallized from an early phase of Aeolian magmatism of tholeiitic composition. Although both interpretations are possible, the accumulated data show that the markedly "tholeiitic" affinity of the Lipari clinopyroxene may be ascribed to a significant contribution from crustal material. For example, the samples with low *V*(*M*2)/*V*(*M*1) value belong to group B (Fig. 5), which contains high-K andesites (Table 1). High-K andesite contains cordierite and shows macroscopic evidence of contamination by material from the low and middle continental crust (Barker 1987, Crisci *et al.* 1991). This inference is confirmed by the presence of interstitial rhyolitic glass in sample L13. Therefore, according to Crisci *et al.* (1991) and Esperança *et al.* (1992), the structural data of the clinopyroxene indicate an important contribution of crustal material in the genesis of magmas at Lipari.

ACKNOWLEDGEMENTS

Authors are grateful to F. Hawthorne, R.F. Martin and W.H. MacLean for their careful revision of the manuscript, and to E.M. Piccirillo for his stimulating discussion. This research was supported by CNR, Centro di Studi per la Geodinamica Alpina, Padova (G.M.) and the Italian M.U.R.S.T. (40% funds to P.F.Z. and 60% funds to G.M.). The English text was revised by G. Walton.

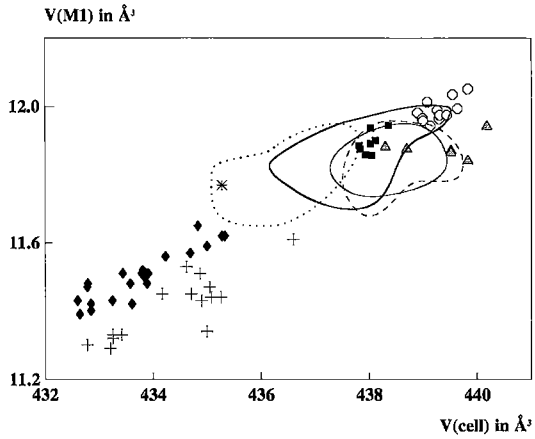

FIG. 4. *V*(*M*1) *versus V*(cell); symbols as in Fig. 1. Bold line: Salina clinopyroxene, dotted line: Filicudi clinopyroxene, solid line: Vulcano clinopyroxene, dashed line: Stromboli clinopyroxene, diamonds: clinopyroxene in nodules of spinel lherzolitic (Dal Negro *et al.* 1984), crosses: clinopyroxene megacrysts in the stability field of spinel, from alkaline rocks (Dal Negro *et al.* 1989), star: high-pressure synthetic clinopyroxene (Manoli & Molin 1988).

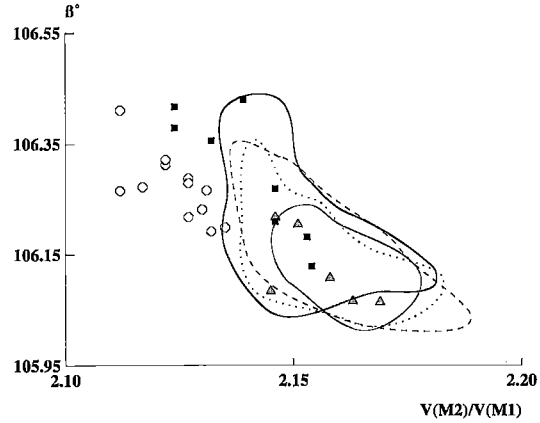

FIG. 5. The angle β *versus* *V*(*M*2)/*V*(*M*1); symbols as in Figures 1 and 4.

REFERENCES

BARKER, D.S. (1987): Rhyolites contaminated with metapelite and gabbro, Lipari, Aeolian Islands, Italy: products of lower crustal fusion or of assimilation plus fractional crystallization? *Contrib. Mineral. Petrol.* **97**, 460-472.

BECCALUVA, L., GABBIANELLI, G., LUCCHINI, F., ROSSI, P.L. & SAVELLI, C. (1985): Petrology and K/Ar ages of volcanics dredged from the Eolian seamounts: implications for geodynamic evolution of the southern Tyrrhenian basin. *Earth Planet. Sci. Lett.* **74**, 187-208.

CARBONIN, S., DAL NEGRO, A., MOLIN, G.M., MUNNO, R., ROSSI, G., LIRER, L. & PICCIRILLO, E.M. (1984): Crystal chemistry of Ca-rich pyroxenes from undersaturated to oversaturated trachytic rocks, and their relationships with pyroxenes from basalts. *Lithos* **17**, 191-202.

CLARK, J.R., APPLEMAN, D.E. & PAPIKE, J.J. (1969): Crystal-chemical characterization of clinopyroxenes based on eight new structure refinements. *Mineral. Soc. Am., Spec. Pap.* **2**, 31-50.

CRISCI, G.M., DE ROSA, R., ESPERANÇA, S., MAZZUOLI, R. & SONNINO, M. (1991): Temporal evolution of a three component system: the island of Lipari (Aeolian Arc, southern Italy). *Bull. Volcanol.* **53**, 207-221.

DAL NEGRO, A., CARBONIN, S., DOMENEGHETTI, C., MOLIN, G.M., CUNDARI, A. & PICCIRILLO, E.M. (1984): Crystal chemistry and evolution of the clinopyroxene in a suite of high pressure ultramafic nodules from the Newer Volcanics of Victoria, Australia. *Contrib. Mineral. Petrol.* **86**, 221-229.

_____, _____, MOLIN, G.M., CUNDARI, A. & PICCIRILLO, E.M. (1982): Intracrystalline cation distribution in natural clinopyroxenes of tholeiitic, transitional and alkaline basaltic rocks. *In* Advances in Physical Geochemistry **2** (S.K. Saxena, ed.). Springer-Verlag, New York, N.Y. (117-150).

_____, MANOLI, S., SECCO, L. & PICCIRILLO, E.M. (1989): Megacrystic clinopyroxenes from Victoria (Australia): crystal chemical comparisons of pyroxenes from high and low pressure regimes. *Eur. J. Mineral.* **1**, 105-121.

_____, MOLIN, G.M., SALVIULO, G., SECCO, L., CUNDARI, A. & PICCIRILLO, E.M. (1989): Crystal chemistry of clinopyroxene and its petrogenetic significance: a new approach. *In* The Lithosphere in Italy (A. Boriani, M. Bonafede, G.B. Piccardo & G.B. Vai, eds.). Advances in Earth Science Research. *Accademia Nazionale dei Lincei* **80**, 271-295.

ESPERANÇA, S., CRISCI, G.M., DE ROSA, R. & MAZZUOLI, R. (1992): The role of the crust in the magmatic evolution of the island of Lipari (Aeolian Island, Italy). *Contrib. Mineral. Petrol.* **112**, 450-462.

FARAONE, D., MOLIN, G. & ZANAZZI, P.F. (1988): Clinopyroxenes from Vulcano (Aeolian Islands, Italy): crystal chemistry and cooling history. *Lithos* **22**, 113-126.

INTERNATIONAL TABLES FOR X-RAY CRYSTALLOGRAPHY **IV** (1974): Kynoch Press, Birmingham, U.K.

MALGAROTTO, C., MOLIN, G. & ZANAZZI, P.F. (1993): Crystal chemistry of clinopyroxenes from Filicudi and Salina (Aeolian Islands, Italy). Geothermometry and barometry. *Eur. J. Mineral.* **5**, 915-923.

MANOLI, S. & MOLIN, G.M. (1988): Crystallographic procedures in the study of experimental rocks: X-ray single-crystal structure refinement of *C2/c* clinopyroxene from lunar 74275 high-pressure experimental basalt. *Mineral. Petrol.* **39**, 187-200.

NIMIS, P. (1995): A clinopyroxene geobarometer for basaltic systems based on crystal-structure modeling. *Contrib. Mineral. Petrol.* **121**, 115-125.

NORTH, A.C.T., PHILLIPS, D.C. & MATHEWS, F.S. (1968): A semi-empirical method of absorption correction. *Acta Crystallogr.* **A24**, 351-359.

PASQUAL, D., MOLIN, G. & ZANAZZI, P.F. (1995): Crystal chemistry of Stromboli clinopyroxene: a comparison with analogues from other Aeolian Islands (Italy). *Eur. J. Mineral.* **7**, 369-378.

PICHLER, H. (1980a): The island of Lipari. *Rend. Soc. It. Mineral. Petrol.* **36**, 415-440.

_____ (1980b): The Aeolian Islands – Carte geologiche. *Rend. Soc. It. Mineral. Petrol.* **36**(1).

ROSSI, G., OBERTI, R., DAL NEGRO, A., MOLIN, G.M. & MELLINI, M. (1987): Residual electron density at the *M2* site in *C2/c* clinopyroxenes: relationships with bulk chemistry and sub-solidus evolution. *Phys. Chem. Minerals* **14**, 514-520.

_____, SMITH, D.C., UNGARETTI, L. & DOMENEGHETTI, M.C. (1983): Crystal-chemistry and cation ordering in the system diopside–jadeite: a detailed study by crystal structure refinement. *Contrib. Mineral. Petrol.* **83**, 247-258.

SALVIULO, G. & MOLIN, G.M. (1993): Crystal-chemistry of clinopyroxene from Sunda volcanic arc. *Mineral. Petrol.* **49**, 233-248.

TOKONAMI, M. (1965): Atomic scattering factor for O^{2-}. *Acta Crystallogr.* **19**, 486.

Received July 2, 1997, revised manuscript accepted November 12, 1997.